

行政院國家科學委員會專題研究計畫 期中進度報告

多埠微波網路量測技術之建立及應用(1/3)

計畫類別：個別型計畫

計畫編號：NSC92-2213-E-002-071-

執行期間：92年08月01日至93年07月31日

執行單位：國立臺灣大學電信工程學研究所

計畫主持人：瞿大雄

報告類型：精簡報告

處理方式：本計畫可公開查詢

中 華 民 國 93 年 5 月 31 日

行政院國家委員會專題研究計畫期中進度報告

多埠微波網路量測技術之建立及應用(1/3)

Development and application of multiport microwave network measurement techniques (1/3)

計畫編號：NSC92-2213-E-002-071

執行期限：92年8月1日至93年7月31日

計畫主持人：瞿大雄教授 國立台灣大學電信工程學研究所

一、 中文摘要

本計畫為一三年計畫(92年至95年)，進行「多埠微波網路量測技術之建立及應用」研發工作。本計畫之重點有三：一為建立「多埠激發-多埠接收法」於多埠網路量測之理論推導及分析公式。二為建立「多埠激發-多埠接收法」之多埠校準器及校準公式。三為應用「多埠激發-多埠接收法」於多埠晶片、電路、微波影像及天線特性量測。

本報告係敘述第一年之研究成果，包含「二埠激發-二埠接收法」於二埠晶片S-參數量測技術，三埠網路分析儀之三埠校準器及校準公式推導，以及建立「多埠激發法」於微波影像之應用。

關鍵詞：多埠微波網路量測技術、校準、微波影像。
英文摘要

This is a three-year project (from 92/8 to 95/7) to conduct researches on multiport microwave network measurement techniques. The major tasks of this project are the following three items. The first item is to develop the basic principle of “multiport-stimulus and multiport-receiving method”. The second item is to develop the calibration method and calibrators for a multiport network network analyzer. The third item is to develop the applications on MMIC, circuit, microwave imaging and antenna measurements using “multiport-stimulus and multiport-receiving method”.

In this first-year report, the study results are mainly focused on the development of a new test set with 2-port stimulus for on-wafer S-parameter measurement, a novel calibration method for 3-port vector network analyzer using 3-port calibrators, and the microwave diversity imaging of conducting objects using multi-source illumination.

Keywords: multiport-stimulus and multiport-receiving method, calibration, microwave imaging.

二、 計畫緣由與目的

In conventional S-parameter test set, such as HP

8516, a 1-port stimulus is switched for forward and reverse measurements, respectively. In this report, we propose a new design of test set without RF switch. In this approach, it uses 2-port stimulus to excite the 2-port DUT simultaneously. Multiple sets of reflection and transmission signals caused by incident signals with different amplitude or phase are then recorded. To eliminate the systematic errors, the TAN self-calibration procedure [1], [2] using three 2-port calibrators is developed for the on-wafer broadband system calibration.

In [3], a general formulation of through-short-delay (TSD) calibration method for multi-port VNA calibration is presented and experimentally demonstrated that a 3-port VNA can be calibrated using a 2-port “through” calibrator and an 1-port sliding load with sexless connectors. In this report, a novel approach to use three 3-port calibrators extended from 2-port through-attenuation-network (TAN) calibrators [4] is developed to calibrate a 3-port VNA.

Microwave imaging is an approach to reconstruct the scattering object characteristics from the recorded object scattered field in the microwave frequency range. For the microwave imaging of conducting objects, frequency and receiving angle diversity techniques have been applied in the bistatic arrangement [5]. In this report, we extend the bistatic frequency-swept microwave imaging system for single-source illumination to the case of multi-source illumination. The reconstructed image then gives an image corresponding to the induced surface current distribution on the illuminated region due to the specular diffraction observed by a linear receiving array. As the results, the multi-source illumination will enlarge the illuminated region on the scattering object surface hence to improve the

resulting image aspect angle.

三、研究方法及成果

I. Novel 3-port Calibration Method

The schematics of the developed three 3-port calibrators are shown in Fig.1, a resistive power divider as a “3-port through”, three 20 dB attenuators connected with the “3-port through” as a “3-port attenuation network”, and a “3-port high reflection network” consisting of three 1kΩ resistors. The error model of a 3-port VNA without leakage errors then consists of the actual 3-port scattering matrix of the DUT S_a , a virtual error box T in terms of transmission parameters and ideal 3-port VNA.

Each error box is defined by the scattering matrix as

$$E_i = \begin{bmatrix} e_i^{11} & e_i^{12} \\ e_i^{21} & e_i^{22} \end{bmatrix}, i=1,2,3. \quad (1)$$

The relationship of input-output signals and the error T -parameter matrix is defined as

$$\begin{bmatrix} b_4 \\ b_3 \\ b_6 \\ a_4 \\ a_5 \\ a_6 \end{bmatrix} = \begin{bmatrix} t_{11} & 0 & 0 & t_{14} & 0 & 0 \\ 0 & t_{22} & 0 & 0 & t_{25} & 0 \\ 0 & 0 & t_{33} & 0 & 0 & t_{36} \\ t_{41} & 0 & 0 & t_{44} & 0 & 0 \\ 0 & t_{52} & 0 & 0 & t_{55} & 0 \\ 0 & 0 & t_{63} & 0 & 0 & t_{66} \end{bmatrix} \begin{bmatrix} a_1 \\ a_2 \\ a_3 \\ b_1 \\ b_2 \\ b_3 \end{bmatrix} = \begin{bmatrix} T_1 & T_2 \\ T_3 & T_4 \end{bmatrix} \begin{bmatrix} a_3 \\ b_1 \\ b_2 \\ b_3 \end{bmatrix}. \quad (2)$$

The scattering matrix measured by the ideal 3-port VNA can be expressed as

$$S_m = (T_1 S_a + T_2)(T_3 S_a + T_4)^{-1}, \quad (3)$$

where S_m is the measured 3-port scattering matrix and S_a is the DUT 3-port scattering matrix.

Substituting (2) into (3), the embedding equations can be found in a matrix form. Because three 3-port calibrators are used to calibrate a 3-port VNA, three sets of 9 calibration equations are acquired. The 1st, 4th, 5th, 7th and 9th of the first equation set and the 1st, 5th, 9th of the second and third equation sets form 11 linear independent equations for solving the 11 error coefficients. One can then use these error coefficients to acquire the DUT S parameters based on the de-embedding equations from the measured S_{ijm} .

The 3-port uncalibrated and calibrated data of the DUT are measured by an Agilent E5071B VNA with Agilent N4431A electronic calibration module (E-Cal). The DUT used to verify the developed calibration method is an HP 11667B power splitter. The measurement results obtained by a 3-port VNA calibrated using the developed 3-port calibrators are shown in a good agreement with those using E-Cal as in Fig. 2.

II. New Test Set with 2-Port Stimulus

The system block diagram of the new test set is shown in Fig. 3. The power splitter (HP 11667B)

divides the incident power equally for 2-port stimuli whose power levels are controlled by two stepping attenuators (HP 8494B). Two dual directional couplers (HP 11692D) are used to monitor the incident signal into the DUT and the reflect signal outward the DUT. The test fixture is a Cascade Summit 9000 probe station with GSG CPW probes. The frequency down converter (HP 8511) is used to convert the receiving RF signals a_1 , b_1 , a_2 and b_2 to IF signals and linked to the HP 8510C for calculating parameters and displaying measurement results.

The error model of TAN self-calibration method can be expressed as a cascade of three two-port networks (A , T and B^{-1}) as $M = ATB^{-1}$, where M is the measurement matrix, A and B^{-1} are error matrices to be deembeded by the calibration procedure. T is the transmission matrix of the DUT.

In the calibration, three different calibration standards are used to give three measurement matrix equations as $M_1 = AN_1B^{-1}$, $M_2 = AN_2B^{-1}$ and $M_3 = AN_3B^{-1}$. Here N_1 , N_2 and N_3 are the transmission matrices of three calibrators. N_1 is a through line, N_2 is a matched attenuator and N_3 is a resistor with symmetrical property and high reflection coefficients. Both N_2 and N_3 are allowed to have non-reciprocity property. Therefore, there are 5 variables to be evaluated in the self-calibration procedure. In addition, the error matrices of A and B^{-1} have 7 variables to be solved. Therefore, one can use the 12 measurement equations expressed to solve all these 12 variables.

In the on-wafer TAN self-calibration procedure, the “thru”, “10dB attenuator” and “resistor” on the Cascade general-purpose impedance standard substrate (ISS, PN: 102-149) are selected as N_1 , N_2 and N_3 . The DUT is a 20dB attenuator on the same substrate. Figure 4 shows the measurement results of the DUT S_{11} and S_{12} using the new test set with TAN self-calibration compared with those using HP 8516 test set with SOLT calibration.

III. Microwave Imaging using Multi-source Illumination

Figure 5 shows the developed experimental microwave imaging system. It has two horn antennas for simultaneously transmitting swept-frequency microwave signals with power levels controlled by two attenuators. An open-ended WR-90 waveguide is used as a receiving probe, located on a 158 cm long linear

scanner for collecting the object scattered field. In the measurement, the frequency is stepped from 7.5 to 12.5 GHz for 51 frequency points and a total of 128 positions are scanned along the linear scanner.

Figure 6 shows the measured Fourier-space data and their reconstructed images of a metallic cylinder with 15 cm radius. The experimental results are shown in good agreement with the simulation results. The reconstructed image shows an about 60° circular ring image corresponding to the shape of the metallic cylinder.

四、結論與討論

In this report, firstly, three 3-port calibrators are developed to calibrate a 3-port VNA. Its embedding and de-embedding equations for 3-port calibrators are formulated based on the 12-term error model with no-leakage errors. The measurement results demonstrate that the calibration procedure using multi-port calibrators is an effective method to calibrate a multi-port VNA. Secondly, a power splitter and two stepping attenuators are used instead of the switch in the conventional test set to develop a new test set with 2-port stimulus for on-wafer S-parameter measurements. This test set exploits the TAN self-calibration procedure to correct the measurement systematic errors. Because the frequency responses of attenuators at different setting values can be eliminated, the characteristics of the attenuators are allowed to be unknown. This test set may provide a new concept for designing a multi-port vector network analyzer. Thirdly,

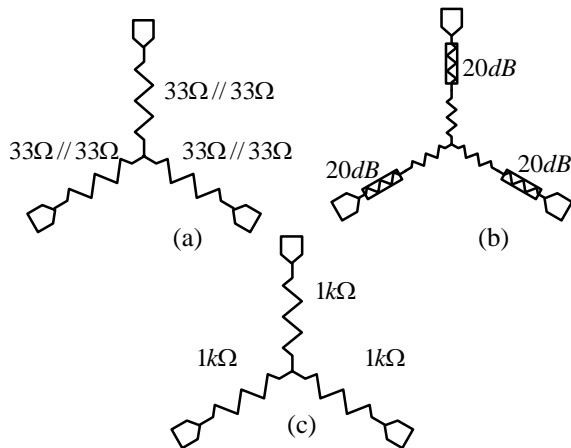


Fig. 1. Schematics of three 3-port calibrators (a) through, (b) attenuation network, and (c) high reflection network.

the bistatic frequency-swept microwave imaging of perfectly conducting objects in a simultaneous multi-source illumination arrangement is experimentally demonstrated. The experimental results shows that using multi-source illumination can provide a cost-effective approach for a wider imaging viewing angle and higher resolution of the scattering object.

五、參考論文

- [1] H. J. Eul and B. Schiek, "A generalized theory and new calibration procedures for network analyzer self-calibration," *IEEE Trans. Microwave Theory and Tech.*, vol. 39, pp.724-731, Apr. 1991.
- [2] C. H. Tseng and T. H. Chu, "On TAN self-calibration for on-wafer S-parameter measurements," 2002 Asia-Pacific Microwave Conference, Kyoto, Japan, Nov. 2002.
- [3] A. Ferrero, F. Sanpietro and U. Pisani, "Multiport vector network analyzer calibration: a general formulation," *IEEE Trans. Microwave Theory and Tech.*, vol. MTT-42, no. 12, pp. 2455-2461, Dec. 1994.
- [4] D. E. Bockelman and W. R. Eisenstadt, "Calibration and verification of the pure-mode vector network analyzer," *IEEE Trans. Microwave Theory and Tech.*, vol. MTT-46, no. 7, pp. 1009-1012, July 1998.
- [5] N. H. Farhat, "Microwave diversity imaging and automated target identification based on models of neural networks," *Proc. IEEE*, vol.77, no.5, pp.670-680, 1989.

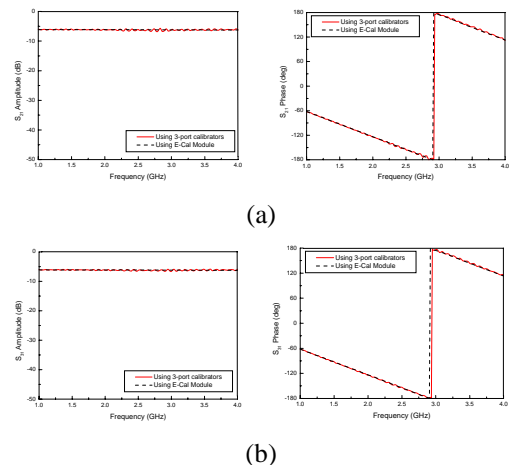


Fig. 2 Measured results of the DUT (a) $|S_{21}|$, (b) $\angle S_{21}$, (c) $|S_{31}|$ and (d) $\angle S_{31}$ using the developed 3-port calibration method with 3-port calibrators in comparison with those using 2-port calibration method with E-Cal module.

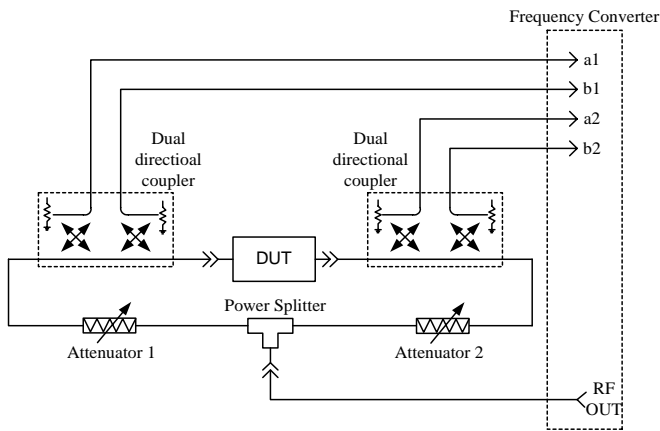


Fig. 3. System block diagram of the new test set with 2-port stimulus for on-wafer S-parameter measurement.

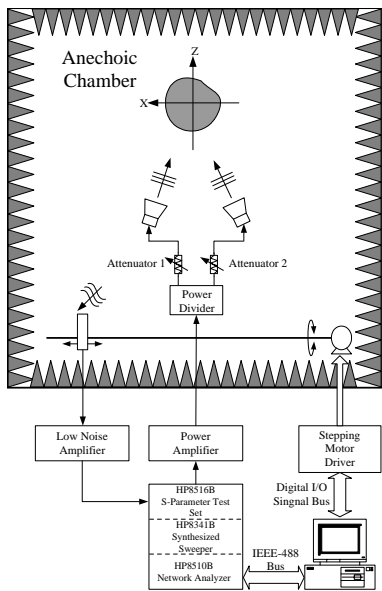
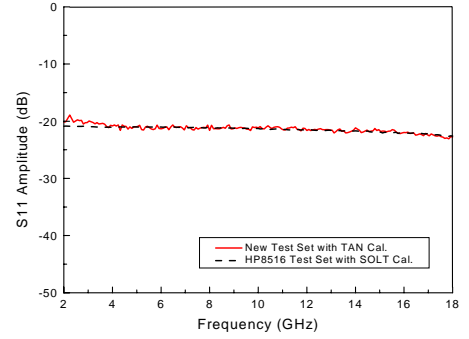
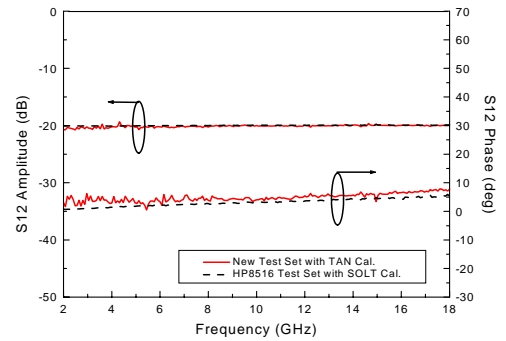


Fig. 5. An automated wide-band bistatic microwave imaging scattering measurement system using multi-source illumination.

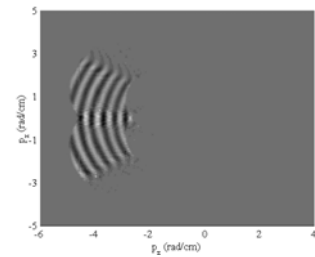


a)

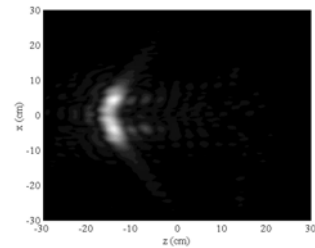


b)

Fig. 4. Measurement results of DUT (a) S_{11} and (b) S_{12} using new test set with TAN self-calibration compared with those using HP 8516 test set with SOLT calibration.



(a)



(b)

Fig. 6. Measured results of Fourier space data and reconstructed images of a metallic cylinder with 15 cm radius.